ISA Transactions xxx (xxxx) xxx

Contents lists available at ScienceDirect

ISA Transactions

journal homepage: www.elsevier.com/locate/isatrans

Research article

Research on optimal control strategy of wind–solar hybrid system based on power prediction ☆

Shu Liu [a,*], Hongyu You [b], Yan Liu [b], Wanfu Feng [b], Shuo Fu [b]

[a] School of Renewable Energy, Shenyang Institute of Engineering, Shenyang, Liaoning, 110136, China
[b] Graduate Department, Shenyang Institute of Engineering, Shenyang, Liaoning, 110136, China

ARTICLE INFO

Article history:
Received 2 February 2021
Received in revised form 8 May 2021
Accepted 8 May 2021
Available online xxxx

Keywords:
Control strategy
Maximum power tracking control
Power prediction
Wind–solar hybrid system

ABSTRACT

In wind and solar power generation systems, the MPPT algorithm is often used to quantify renewable energy production power, if the light or wind changes suddenly in the algorithm search process, it is possible that the iterative algorithm will not be able to track to the maximum power point or fall into turbulence, and frequent restart of the relevant algorithm will also bring a large energy loss. In view of this situation. For the purpose of further analysis the effect of power output characteristics on the tracking ability of the system, and to enhance the reliability and energy utilization of renewable energy generation system. This manuscript studies an optimal control method for a wind–solar storage complement device designed using power prediction. The article establishes the simulation model of each subsystem separately, and the wavelet packet neural network is used to build a power prediction model. An MPPT optimal control strategy is proposed. This control strategy combines the hysteresis loop comparison-based P&O algorithm in single-peak MPPT and the improved firefly algorithm in multi peak MPPT. The dynamic tracking ability, speed and single peak value and multi peak optimization capability of the algorithm are guaranteed. And the simulation analysis of the control strategy is executed by MATLAB, and the findings demonstrate the efficacy of the optimum control technique proposed in this article. This algorithm has also been shown to outperform traditional intelligent algorithms in terms of tracking efficiency and stability

1. Introduction

Wind energy and solar energy both have distinct resource characteristics, which makes the characteristics of wind power generation and photovoltaic power generation have natural complementarity, the multi-energy complementary power generation system in the same area has greater ascendant than the single-energy power generation system. How to further improve the wind–solar utilization rate, optimize the energy structure and related technologies while ensuring the system stability is a hot issue in the industry [1–3].

Wind and solar energy are affected by the environment with uncertainty [4–6]. The random change of wind speed or partial shading of solar cells can easily cause the mismatch of solar array, which has an effect on the power output of wind turbines and photovoltaic power generation systems. MPPT is an efficient method of using wind and solar energy. It can enhance the generation efficiency of renewable energy sources [7,8], so that they can output more energy in the event of fluctuations or disturbances in the external environment. The common single peak MPPT algorithms include disturbance observation method [9], incremental conductance method [10] and fuzzy algorithm [11]. The tracking effect of these algorithms is not ideal when facing the multi peak power curve. If the light or wind speed mutation occurs in the algorithm search process, it is easy to fall into local extremum or oscillation. For this reason, some scholars proposed multi peak MPPT algorithm, such as particle swarm MPPT [12,13], neural network MPPT [14] and firefly MPPT algorithm [15]. However, if only relying on the simple multi-peak MPPT algorithm, when the algorithm is stable, it needs to judge the environmental change by power fluctuation and restart the algorithm. If the algorithm is restarted frequently, when the maximum power point position changes little, the energy will be lost greatly.

For further improve the power tracking ability of MPPT algorithm, many scholars study and analyze it combined with power prediction. A new variable step conductivity increment method MPPT based on power prediction is presented in the reference [16]. This programme adopts a new step adjustment coefficient, which can adjust the step according to the change of

☆ **Funding** This work was supported in part by the Key research and development program of Liaoning Provincial Department of science and Technology [grant numbers 2019JH8/10100064]; the Scientific research project of Liaoning Provincial Department of Education [grant numbers JL-2014].

* Corresponding author.
E-mail address: ls_jhl@163.com (S. Liu).

https://doi.org/10.1016/j.isatra.2021.05.010
0019-0578/

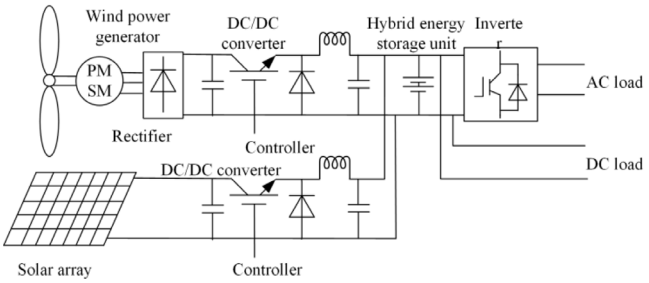

Fig. 1. Structure of Scenery Complementary System.

external conditions, and solves the contradiction between tracking speed and steady-state accuracy. A variable duty cycle step disturbance method on account of the combination of fuzzy control and power prediction is studied to track the maximum power of the system [17]. Simulation and comparison show that this method has good performance in tracking speed, stability and maximum output power. Compensation voltage is obtained by using the relationship between maximum output power and corresponding control voltage variation. By improving the variable step P&O algorithm based on power prediction, the maximum power tracking is realized, which improves the tracking speed, stability and accuracy [18].

To address the above issues and studies, in order to further improve the reliability and energy utilization of renewable energy generation systems, the impact of power forecasting on MPPT process of the system is combined. In this paper, by taking the complementary system of wind–solar storage as the research object, a power prediction model of wind–solar storage system based on WPNN is established. On this basis, a tracking technique based on MPPT is proposed for an optimized wind–solar storage system, which combines disturbance observation method based on hysteresis comparison (HCDOM) in single-peak MPPT and improved fluorescent algorithm (IFA) in multi-peak MPPT. It further guarantees the system's dynamic tracking ability, speed and the ability to optimize multi-peak and single-peak values. Finally, in the simulink environment, each subsystem is modeled and the control policy is simulated and analyzed. The effectiveness of the control strategy proposed in this manuscript and the rationality of the system design can be obtained from the simulation results.

2. The complementary device designed for wind–solar-storage

Wind power is characterized by weak wind speed in the daytime but strong wind speed at night, while solar energy is on the contrary, with strong light in the daytime but weak light at night. Both of them form a natural complementary effect due to their own resource characteristics and power generation characteristics. To enhance the utilization of energy, this device's energy storage component employs a hybrid energy storage system, and its energy storage unit is made up of super capacitor and battery. The control system includes wind turbines, solar cells, rectifiers, controllers, converters, hybrid energy storage units and loads.The composition of the control system is revealed in Fig. 1.

2.1. Wind power generation model

Build simulation model of wind energy utilization coefficient, wind turbine model and wind power generation sub-system model in Matlab/Simulink.

The simulation model is a wind power subsystem in Fig. 2, including wind turbine sub-module, improved firefly algorithm simulation model and boost circuit simulation model. The input quantities of the wind turbine sub-module are input wind speed, wind wheel radius, pitch angle, and generator speed, and the output quantities are output power and output torque. An oscilloscope is connected to the wind energy utilization factor output to obtain the change in Cp value, when the wind speed changes. The MPPT control strategy sends out pulse signals into the booster circuit switching tubes to change the duty cycle and output a higher power DC, when the external wind speed is changing.

2.2. Photovoltaic power generation model

Build a solar cell simulation model in Simulink, as shown in Fig. 3. The I_{sc}, U_{oc}, I_m and U_m of the solar cell are 15 A, 320 V, 12 A and 250 V respectively, and the temperature is set to 25 °C.

The emulation model of the PV power production subsystem is revealed in Fig. 4. The MPPT control process of the PV power generation subsystem is similar to that of the wind power generation subsystem. The MPPT model outputs pulsating signal to change the duty period of DC–DC converter switch to control the output power. The model diagram of the photovoltaic subsystem is shown in Fig. 4.

2.3. Hybrid energy storage unit model

The hybrid energy storage unit is composed of supercapacitors and batteries. The hybrid energy storage unit combines the peculiarities of supercapacitor and battery, and utilizes the merits of high power density and rapid respond speed of supercapacitor, which can avoid the disadvantage of insufficient energy storage capacity. The supercapacitor undertakes the part with frequent fluctuations in the total power, and the battery undertakes the relatively smooth part of the total power. This combination can reduce the small cycle charging and discharging phenomenon caused by frequent charging and discharging, improve the battery's charging and discharging phase, so that the battery's service life is extended and the system's maintenance costs are reduced. The supercapacitor and battery are linked to the DC bus with a DC/DC adapter. Fig. 5 depicts the circuit chart of the released hybrid energy storage device.

In the figure, V_B is the battery voltage; R_B is the battery's equal internal resistance; L is the bidirectional DC/DC converter's inductance; S_i and D_i is the power switching device, $s = 1, 2$; C is the DC bus capacitance; V_{UC} is the super capacitor bank's equivalent ideal voltage source; R_{UC} is the equivalent internal resistance of the super capacitor bank; R_{CPL} is the equivalent constant power load.

Assuming that the time to turn on S_1 or turn on D_1 is d and the inductance current i_L and perfect capacitor voltage u_c are state variables, the equation of state is obtained as follows:

$$\begin{cases} L\dfrac{di_L}{dt} = V_B - du_C - R_B i_L \\ C\dfrac{du_C}{dt} = di_L + \dfrac{V_{UC} - u_C}{R_{UC}} - \dfrac{u_C}{R_{CPL}} \end{cases} \tag{9}$$

where R_{CPL} is the constant power load, when the load power is P_0, $R_{CPL} = {u_c}^2/P_0$.

2.4. Simulation model of wind and light storage power generation system

The wind–solar hybrid power generation system model in Simulink, as seen in Fig. 6.

To verify the complementarity of this system, the DC side current is inverted by the inverter to supply the AC load with double 3kw AC load powers, and the fluctuation of the load power is simulated by the shutdown of the three-phase circuit

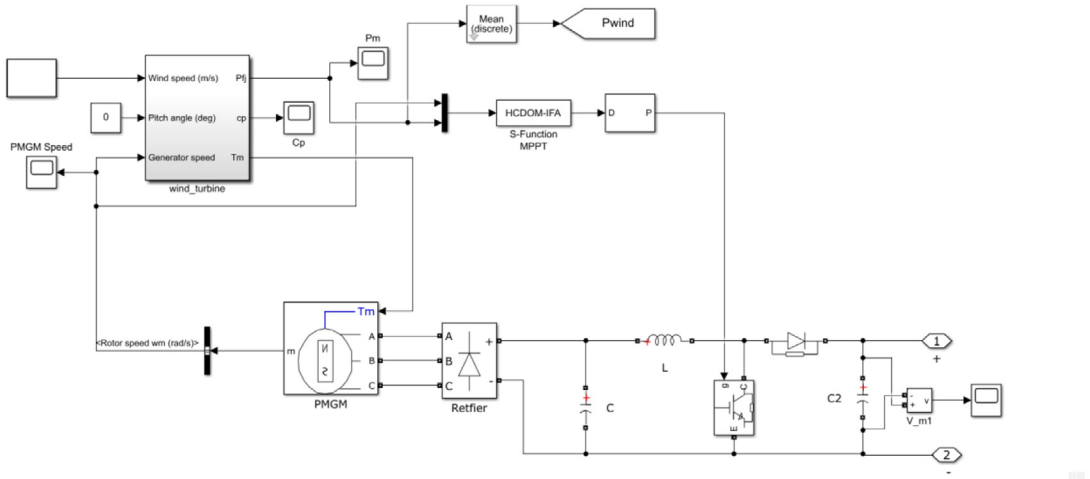

Fig. 2. Simulation model of wind power subsystem.

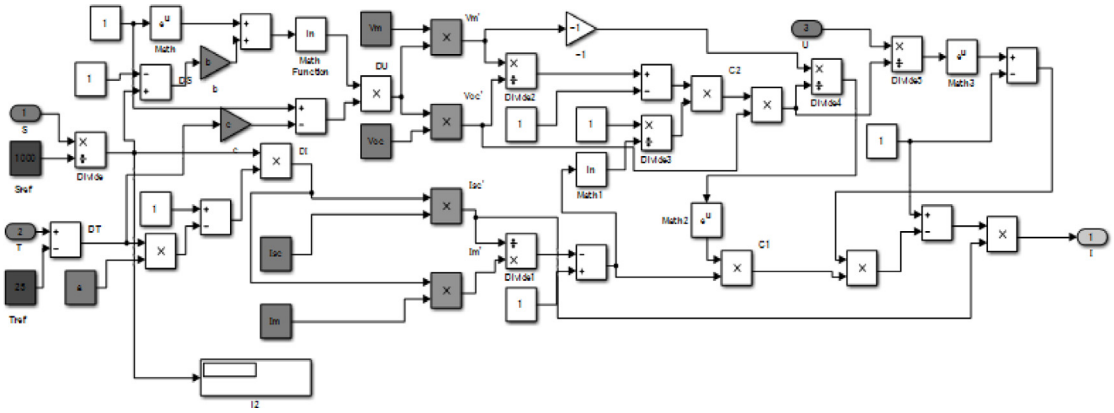

Fig. 3. Solar cell simulation sub-module.

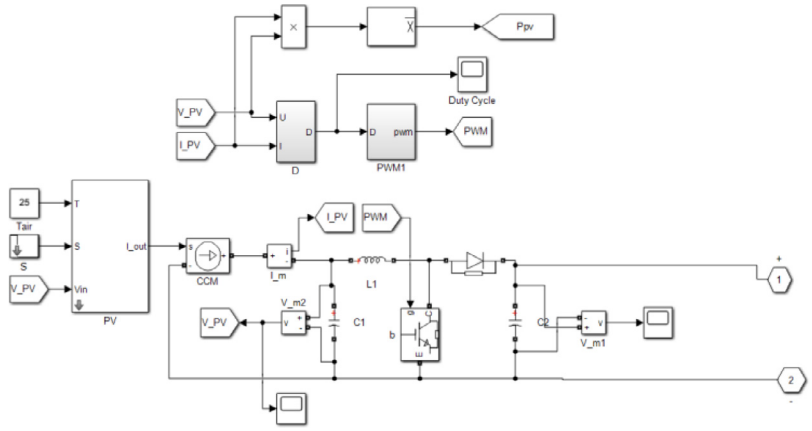

Fig. 4. Photovoltaic subsystem simulation model.

breaker. The simulation of the total system under the assumed environmental changes is shown in Fig. 7.

From the top to the bottom of the simulation curve are the rated power of AC load, the export power of PV, wind power generation subsystems , the charging and discharging of the combined energy storage system, which shows that between 0 s and 1 s, the wind power generation subsystem emits 5.2 KW and the PV power generation subsystem emits 3.2 KW, of which 3.2 KW is supplied to the grid and 5.2 KW is supplied to the energy storage system. Between 1 s and 2 s, the irradiance suddenly drops, and the 8.4 KW issued by wind power generation and photovoltaic power generation two subsystems are allocated to the grid and the energy storage system. Between 2 s and 3 s, the power required by the load becomes 6 KW, the wind speed suddenly drops, the wind speed is smaller than the wind speed at which the cut-in occurs, the wind power generation subsystem stops, and the power issued by the photovoltaic power generation subsystem is 2.5 KW, which cannot meet the demand of the grid. The remaining part is supplemented utilizing an electricity

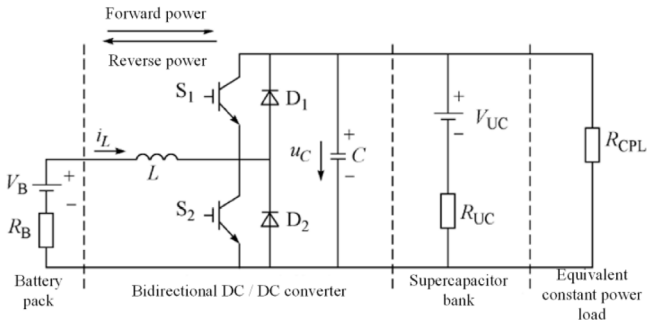

Fig. 5. Equivalent circuit of hybrid energy storage system.

storage device. For the remaining time, the simulation results change little.

It is evident that the wind and solar power system designed in this manuscript can output smooth power when the external environment changes suddenly.

3. Power prediction model of WPNN

Enhancing the power prediction accuracy of wind–solar hybrid system is helpful to improve the security and economy of power system. This paper adopts WPNN for power prediction of wind and solar complementary systems. Wavelet analysis has advantages in extracting signal features and analyzing non-stationary signals. Combining with the self-adaptive ability of artificial neural network, strong self-learning ability and powerful multi factor fuzzy problem, the prediction accuracy of the model can be greatly improved. WPNN model has a unique advantage in mapping and forecasting renewable energy output power signals with strong randomness and volatility.

3.1. Model analysis of WPNN

(1) Wavelet packet model analysis

Wavelet analysis is a mathematical method, which decomposes signal or function into different frequency components, and then analyzes each component according to its scale and resolution. The time–frequency characteristics of renewable energy output can be obtained by using wavelet transform, and then the output components of renewable energy output in different time scale change periods can be obtained by analyzing the time–frequency characteristics. In multi-scale analysis, the relationship between scale function and wavelet function is as follows:

$$\phi(t) = \sqrt{2}\sum_{k=-\infty}^{\infty} h_k \phi(2t-k) \tag{10}$$

$$\psi(t) = \sqrt{2}\sum_{k=-\infty}^{\infty} g_k \psi(2t-k) \tag{11}$$

where h_k and g_k are the filter coefficients.

According to the theory of wavelet packet analysis, wavelet decomposition algorithm and reconstruction algorithm can be expressed as follows

$$d_k^{(j+1,2n)} = \frac{1}{\sqrt{2}}\sum_l \overline{h_{l-2k}} d_l^{(j,n)} \tag{12}$$

$$d_k^{(j+1,2n+1)} = \frac{1}{\sqrt{2}}\sum_l \overline{g_{l-2k}} d_l^{(j,n)} \tag{13}$$

$$d_k^{(j,n)} = \sum_l \left(h_{k-2l} d_l^{(j+1,2n)} + g_{k-2l} d_l^{(j+1,2n+1)}\right) \tag{14}$$

where $d_k^{(j,n)}$ is wavelet packet coefficients; $d_k^{(j+1,2n)}$ and $d_k^{(j+1,2n+1)}$ are wavelet packet decomposition coefficients; ; h_{k-2l} and g_{k-2l} are reconstructed low-pass filters and high-pass filters by wavelet packet severally.

(2) BP neural network

BP neural network is a kind of neural network with forward propagation for results and backward propagation for errors. Input layer, hidden layer and output layer are the main structures. Each department has its own different functions, receiving data through the input layer, output layer output data. The former layer of neurons connect to the next layer of neurons and collect the information from the upper layer of neurons. The value is passed to the next layer through activation.

It can be obtained from Fig. 8, the input net_i and output o_i of the ith node in the hidden layer and the input net_k and output o_k of the kth node in the output layer can be expressed as follows:

$$net_i = \sum_{j=1}^{M} w_{ij} x_j + \theta_i \tag{15}$$

$$o_i = \phi(net_i) = \phi\left(\sum_{i=1}^{M} w_{ij} x_j + \theta_j\right) \tag{16}$$

$$net_k = \sum_{i=1}^{q} w_{ki} \phi\left(\sum_{i=1}^{M} w_{ij} x_j + \theta_j\right) + \alpha_k \tag{17}$$

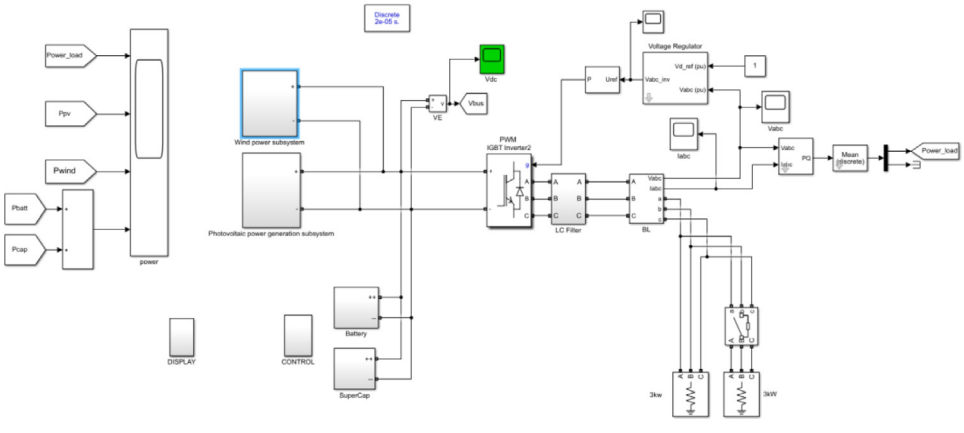

Fig. 6. Simulation model of wind and light storage power generation system.

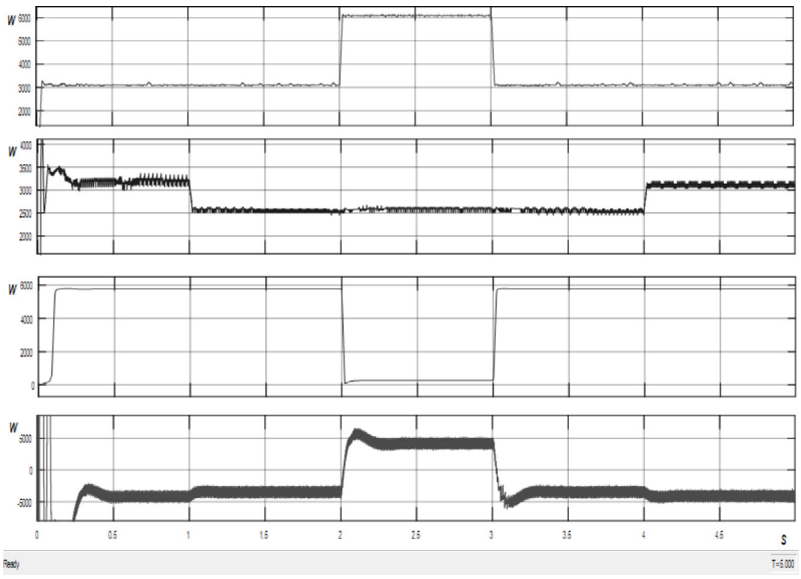

Fig. 7. Wind–solar hybrid power supply system simulation curve.

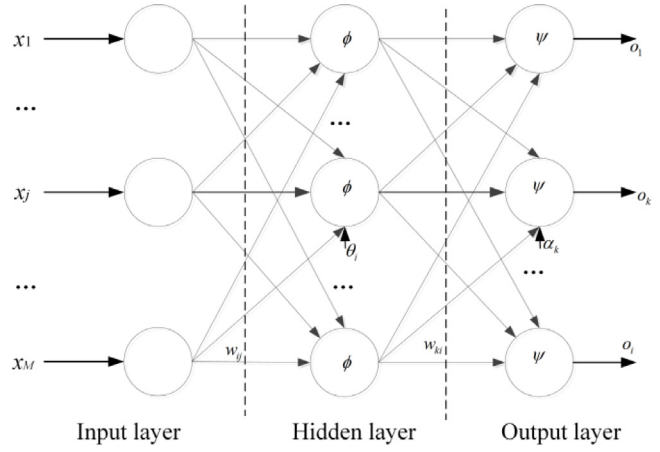

Fig. 8. A typical three-layer BP neural network.

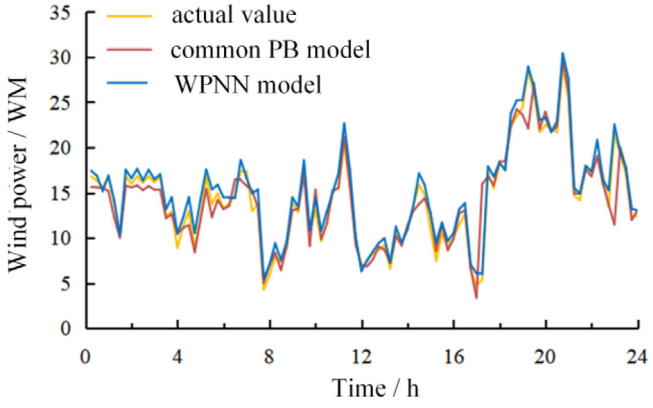

Fig. 9. Wind power forecast.

$$o_k = \psi(net_k) = \psi\left[\sum_{i=1}^{q} w_{ki}\phi\left(\sum_{i=1}^{M} w_{ij}x_j + \theta_j\right) + \alpha_k\right] \tag{18}$$

where x_j is the input of the input layer's jth node; w_{ij} is the weight between the ith node of hidden layer and the jth node of input layer; θ_i is the ith node threshold in the hidden layer.; ϕ is the excitation function of the hidden layer; w_{ki} is the weight between the kth node in the output layer and the ith node in the hidden layer; α_k denotes the threshold of the kth node in the output layer; M is the dimension of the input signal; q is the total number of nodes in the hidden layer; L is the node dimension of the output layer; ψ is the incentive function of the output layer.

3.2. Power prediction model of wind–solar hybrid generation system based on WPNN

The power prediction of wind–solar hybrid power system on account of WPNN is to extract the high-frequency components from the original sequence after wavelet packet decomposition, and obtain the low-frequency components with gentle changes, which makes its characterization characteristics more obvious on the spatial–temporal scale. For improving the ability of mapping the variation characteristics of output power, several BP networks are established to train the high and low frequency components with different variation characteristics. In this article, wavelet packet transform is used to decompose the output power series of wind farm and photovoltaic power station and the related meteorological factors series. Neural networks are established to train and predict the decomposed subsequences, and then the predicted output is reconstructed to obtain the complete power series.

The value of Maximum Relative Error (MRE) and Mean Absolute Percentage Error (MAPE) is used to judge the forecast result

$$MAE = n^{-1}\sum_{i=1}^{n}\left|w_i - w_i'\right| \tag{19}$$

where n represents the number of predicted sample data, w' represents the output value of predicted power of wind farm, and w_i is the wind farm's real generating capacity.

$$MAPE = n^{-1}\sum_{i=1}^{n}\left|y_i - y_i'\right| \cdot y_i^{-1} \times 100\% \tag{20}$$

where, n is the number of predicted sample data; y_i' is the predicted wind's worth farm predicted power; y_i is the real value of wind farm actual power generation.

4. MPPT control strategy

MPPT control is to continuously sample the output power of wind turbines or photovoltaic cells, and use different types of power electronic conversion circuits to obtain the maximum output power corresponding to the external environmental conditions by changing the load impedance to adapt to the changing environmental conditions.

In the MPPT tracking control process, the system is generally in a state of no extra large disturbance. If there is a big mutation or interference in the light or wind in the search process of the algorithm, the sampling data and iterative results before the change are easy to fail, resulting in the iterative algorithm cannot discover the global maximum power point or fall into the oscillation that cannot converge. Frequent restart of the multi peak algorithm will also bring a lot of energy loss. Aiming at this kind of situation, to overcome the frequent restart of algorithm, energy loss and reduce oscillation caused by the change of system environment, and ensure the dynamic tracking ability, speed and multi peak and single peak optimization ability of the system. Aiming at the firefly algorithm, an improved MPPT control strategy based on hysteresis comparison is proposed. Due to the limitation of space, the disturbance observation method of hysteresis comparison is not introduced in this paper.

4.1. Improved firefly algorithm

(1) Mathematical expression of traditional firefly algorithm

Firefly algorithm (FA) regards every point in space as a firefly, and takes advantage of the characteristic that the Firefly with strong light will attract the Firefly with weak light. In the process of firefly moving, it accomplish the iteration of position, so as to find the first-rank situation and complete the optimization procedure.

In FA algorithm, the degree of attraction β of each firefly can be quantitatively expressed as:

$$\beta = \beta_0 \exp\left(-\gamma r_{ij}^2\right) \tag{21}$$

where β_0 is the initial attraction when r = 0, usually set to 1; r is the interval between two fireflies in Cartesian coordinates; γ is the light absorption coefficient of the medium. The Cartesian size from firefly ith to firefly jth:

$$r_{ij} = \left\|x_i - x_j\right\| = \sqrt{\sum_{k=1}^{d}\left(x_{i,k} - x_{j,k}\right)^2} \tag{22}$$

where $x_{i,k}$ and $x_{j,k}$ are the kth elements of the ith and jth firefly space coordinates. It can be obtained in two-dimensional coordinate system:

$$r_{ij} = \sqrt{\left(x_i - x_j\right)^2 + \left(y_i - y_j\right)^2} \tag{23}$$

If firefly i has firefly j attraction of greater luminosity, the firefly i location can be achieved by Eq. (24).

$$\begin{aligned} x_i(t+1) &= x_i(t) + \beta\left[x_j(t) - x_i(t)\right] \\ &\quad + \alpha(\text{rand} - 1/2) \end{aligned} \tag{24}$$

where α is a constant in the interval [0, 1]; rand is a random number in the range of [0, 1]; $x_i(t)$ and $x_j(t)$ are the positions of the ith and jth fireflies at the current time respectively; and are the updated new positions.

(2) Improved firefly algorithm

In the traditional FA algorithm, if the value of the perturbation step factor α is large, the free step in the position update equation will be large, which will lead to large fluctuations in the voltage and power of the system and make the algorithm exit the convergence state again after the first convergence. If the value of the perturbation step factor α is small, exploring the proximity of high-brightness fireflies can be challenging. In this case, the free step in the original FA iteration equation α (Rand-1/2) is replaced by a variable step function that is positively related to the spacing R, allowing low visibility fireflies to sense the region near the high brightness fireflies more effectively.

The new iterative formula replaces the unknown variables in Eq. (24) α (rand-1/2)

$$x_i(t+1) = x_i(t) + \beta\left[x_j(t) - x_i(t)\right] + S \cdot \text{rand}\{-1, 1\} \tag{25}$$

where rand{−1, 1} means that the probability of −1 and 1 being taken as values in the set is 50%. In addition, the step function s is defined as:

$$S = v\left(1 - \frac{1}{e^m}\right)m + \frac{\text{rand} - 1/2}{5} \tag{26}$$

where v is a constant; (rand-1/2)/5 is the oscillating step, m can be expressed as the ratio of rand $U_{\max}$.

If the fireflies are far away from each other, S takes a larger value, and Low-brightness fireflies can quickly spot high-brightness fireflies. The S meaning is lower if the fireflies are close to one another. To ensure that the static oscillation following algorithm convergence is within a reasonable range, a reasonable upper threshold of s should be set.

4.2. Analysis of the control strategy based on HCDOM-IFA algorithm

Based on power closed loop, the algorithm combines HCDOM and IFA algorithm. HCDOM is used for steady-state operation and dynamic response, and IFA algorithm is used for optimization in case of abrupt multi peak.

Firstly, the algorithm runs HCDOM continuously. If the current environment is in the process of change, it always runs HCDOM to track the extremum until it is judged that the external environment is stable and the working point is at a certain extremum point, and then enters the peak condition judgment link. If the irradiance or wind speed changes slowly, the working point can maintain near the value point, and the energy loss is negligible; when the irradiance or wind speed changes violently, the working point will have a certain offset lag, and it can still track to the extreme point if the irradiance or wind speed is stable. The peak value is determined using the power closed-loop algorithm. It is important to confirm whether the current extreme point is the global maximum power point or whether the current characteristic curve has a single peak value. If it is, it is considered that the search process is over and the HCDOM with small step length will run back to the extremum. Otherwise, according to the voltage range determined by the power closed-loop method, after fast convergence, search for the global maximum power point through the IFA method, it still returns to the steady-state operation of HCDOM.

5. Simulation analysis

5.1. Foundation parameters

To make up for the lack of energy storage in a single battery and to extend the battery life, make full use of supercapacitor

Table 1
Main parameters of scenery complementary system.

Parameter	Unit	Parameter	Unit
P_W	50 kW	I_{sc}	15 A
P_V	30 kW	I_m	12 A
U_m	250 V	V_B	240 V
U_{oc}	320 V	V_{UC}	360 V

Table 2
Key parameters of the MPPT test platform.

Parameter	Unit	Parameter	Unit
Cycle of MPPT	0.5 s	Control period	20 kHz
Inductance of BOOST	2 mH	Input capacitance	10 μF
DC bus capacitance	2240 μF	Resistive load	16 Ω
DC Bus Voltage	385 V	Rated power of platform	1500 W

to make it play a role in hybrid energy storage system. Based on its own characteristics, it undertakes the mismatched high-frequency energy between the power generation system and the energy consumption system. Ultracapacitors, like batteries, are attached to the DC bus via a DC/DC converter. The main parameters of the complementary wind–solar storage system are shown in Table 1. Key parameters of MPPT test platform are shown in Table 2.

5.2. Power prediction analysis of WPNN

To prove the overall validation of WPNN power prediction model, forecasting wind power output series of target wind farm in one day, the data of the certification part of the sample is the measured data of a regional wind farm in Northeast China, and one data is collected every 15 min. The collected data were simulated in MATLAB using the ordinary BP model and the WPNN model, respectively, and the Fig. 9 shows the simulation results. The evaluation of each index is revealed in Table 3.

It can be observed from Fig. 9 and Table 3 that the forecast accuracy of WPNN model is higher than that of BP model, which is closer to the actual value. The prediction error of general BP model to WPNN model is increased by 6.71% and the prediction effect of WPNN model is better.

5.3. Control strategy analysis

The output power of the system is finally derived by simulating the variation of wind speed and light illumination when the HCDOM-IFA algorithm is used.

(1) Photovoltaic system

For photovoltaic system, the light intensity is fixed at 400 W/m in the first 50 s, then increased to 800 W/m, and finally decreased to 600 W/m. Fig. 10 shows the change of light intensity. After using different MPPT control methods, the change of power with light intensity is shown in Fig. 11.

(2) Wind power system

The Fig. 12 shows the wind speed variation diagram. In the first 50 s, where the wind speed is given as 4 m/s in the first 50 s, increases from 4 m/s to 9 m/s from 50 to 100 s, and decreases from 9 m/s to 6 m/s from 100 to 150 s. Fig. 12 shows the wind speed variation. The wind speed variation graph is given in Fig. 12. The variation of power with wind speed after using different methods of MPPT control is shown in Fig. 13.

It can be obtained from Figs. 11 and 13 that for the MPPT control strategy of photovoltaic power generation system and wind power generation system, when MPPT is not used, the output power is low; when IFA is used, the power to ordinary FA is increased by 350 w, and the effect is good; when HCDOM-IFA is used, the effect is the best.

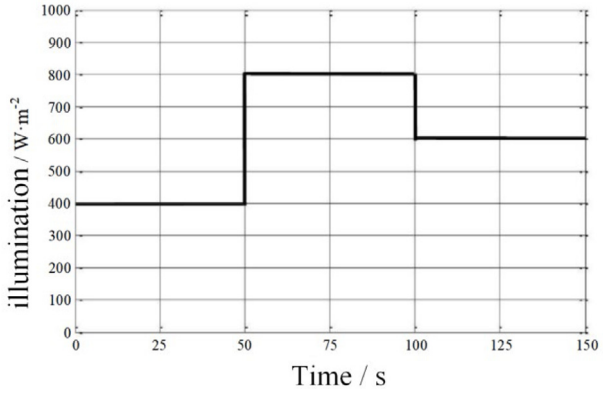

Fig. 10. Variation of light intensity.

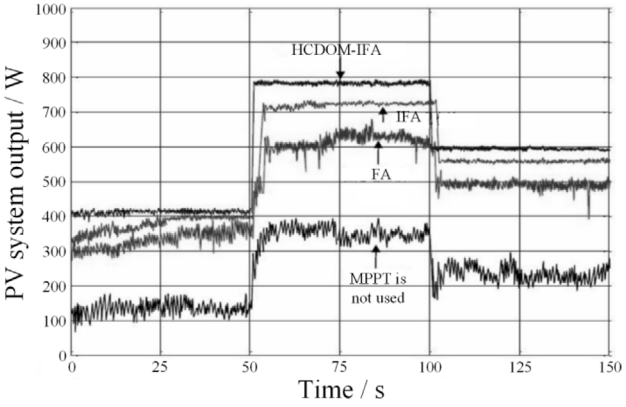

Fig. 11. Power variation diagram with light intensity.

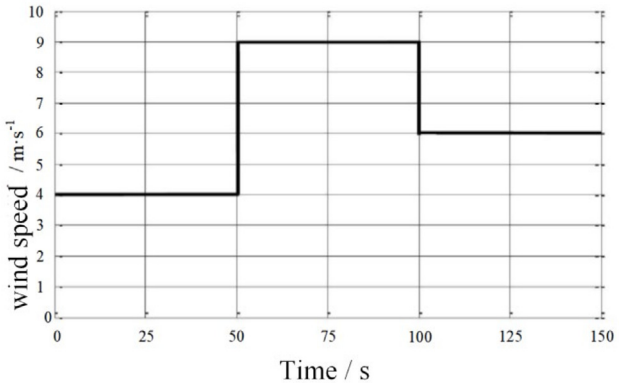

Fig. 12. Wind speed variation diagram.

(3) Analysis of algorithm seeking capability

As the power characteristic curve of PV panel under normal condition and under partial shading is different, specifically its power characteristic curve has only one peak point under normal condition, and when the PV panel is under partial shading, the power characteristic curve has multiple extreme points. In order to simulate the finding ability of this algorithm in both cases the series PV array was built in Simulink environment and its simulation diagram is shown in Fig. 14. The input values for each PV panel are 8.83 A, 36.8 V, 8.3 A and 249 V, the temperature is set to 25 °C. When verifying the algorithm's search for optimality in

Table 3
Evaluation of wind power prediction model.

Model/Index	Maximum absolute error (MAE)	Mean absolute percentage error (MAPE)
Common PB model	89.82%	11.89%
WPNN model	36.29%	5.18%

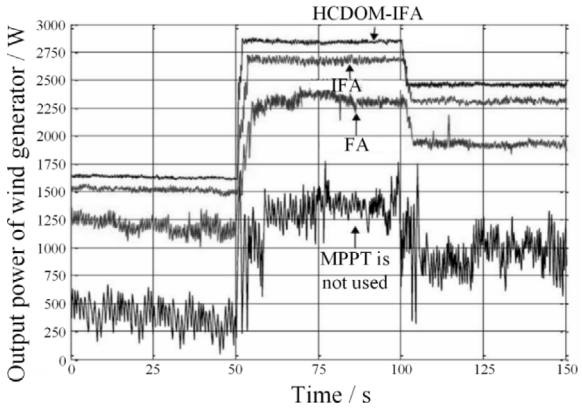

Fig. 13. Wind turbine output power variation diagram.

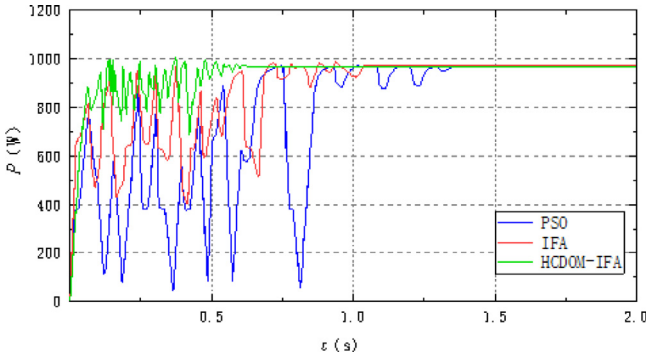

Fig. 15. Power comparison chart in single-peak case.

the single-peak case, the light intensity of each PV panel is 1000. When verifying the optimization of the algorithm in the case of multiple peaks, the light intensity of each panel is set to 500 800 1000 and 1000, other parameters remain unchanged.

The particle swarm algorithm, enhanced firefly algorithm, and HCDOM-IFA algorithm were used to simulate in Simulink case respectively, with the light intensity of each PV panel fixed at 1000 W/m and the temperature set at 25 °C. Fig. 15 depicts the simulation effects. In Fig. 15, all three algorithms finally track to the maximum power, the maximum power of about 970 w, The shortest time for the HCDOM-IFA optimization to track the maximum power is about 0.62 s, while the particle swarm algorithm and the improved firefly algorithm track the maximum power in 1.34 s and 1.07 s, respectively, This shows that the tracking efficiency of this algorithm in the single-peak case is greatly improved compared to the particle swarm algorithm and the improved firefly algorithm. Also from the figure it can be seen that the particle swarm algorithm and the improved firefly algorithm have large power fluctuations in the early stage compared to the HCDOM-IFA algorithm, which also proves that the stability of this optimization is better compared to the other two algorithms.

To simulate the power variation of PV panels under local shading, the light intensity of each PV panel was set to 500 800 1000 and 1000, and the temperature was fixed at 25 °C, the three algorithms mentioned above are still used for simulation comparison in the Simulink environment. Fig. 16 shows the simulation results. It can be obtained from the figure that in the shadow situation, all three algorithms can track the maximum power, but the maximum power decreases to about 637 w compared to the unshaded case, and the time required to trace the maximum power becomes longer. The longest tracking time is 1.47 s for the particle swarm algorithm, 1.26 s for the improved firefly algorithm, and 0.74 s for the shortest tracking time for the HCDOM-IFA algorithm. At the same time, it can be obtained from the figure that the power fluctuation of the HCDOM-IFA algorithm in the process of seeking is significantly smaller than the other two algorithms, and it can be concluded from the above analysis that the tracking efficiency of the HCDOM-IFA algorithm is higher and the stability is better in the case of multiple peaks.

6. Conclusion

Based on the complementarity of wind energy and solar energy in time and space, this paper constructs a wind energy storage complementary power generation system model. This

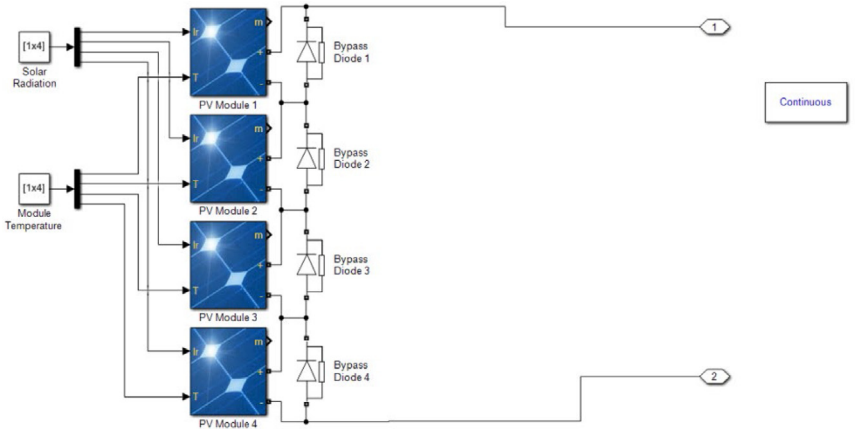

Fig. 14. Series PV array simulation model.

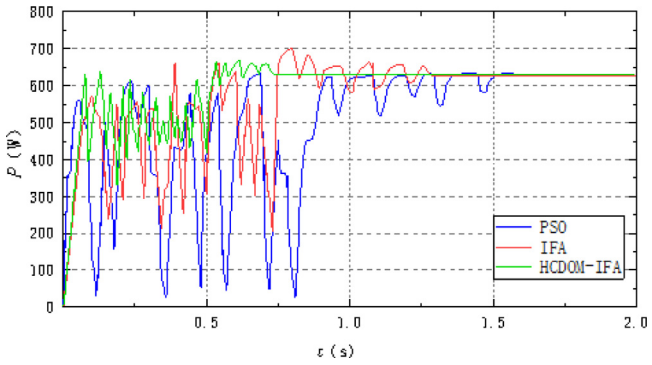

Fig. 16. Multi-peak case power comparison chart.

paper studies the control strategy and power prediction of the system. The control strategy proposed is simulated and analyzed.

(1) Based on the topological structure of wind–solar hybrid power generation system, the hybrid energy storage unit composed of battery and supercapacitor is applied to the wind-complementary system, which improves the stability and flexibility of the wind and photovoltaic hybrid power.

(2) The effect of output power on power tracking characteristics is investigated, and a wavelet packet neural network prediction model is proposed. The model predicts the strength of a wind–solar hybrid system. The Mae and MAPE indexes are used to forecast the model's results.

(3) A MPPT optimal control strategy for complementary wind and solar storage systems is proposed. The control strategy combines the disturbance observation method based on hysteresis comparison in single peak MPPT and the improved firefly algorithm in multi-peak MPPT. The simulation result shows that the method improves the power output, reduces the degree of system oscillation around the MPP, and ensures the dynamic tracking ability, speed, and single peak and multi-peak optimization ability.

Declaration of competing interest

The authors declare that they have no known competing financial interests or personal relationships that could have appeared to influence the work reported in this paper.

References

[1] Tianpei Zhou, Wei Sun. Capacity optimization design of hybrid energy storage unit in wind-solar hybrid power generation system. Acta Sol Energy Sin 2015;36(03):756–62.
[2] Khalid M, Al-Muhaini M, Aguilera RP, Savkin AV. Method for planning a wind–solar–battery hybrid power plant with optimal generation-demand matching. IET Renew Power Gener 12(15):1800–6.
[3] Saeedi M, Moradi M, Hosseini M, et al. Robust optimization based optimal chiller loading under cooling demand uncertainty. Appl Therm Eng 2019;148:1081–91.
[4] Shu Liu. Control and research on blade vibration of wind turbine. Int J Smart Home 2015;9(7):203–12.
[5] Abedinia O, Zareinejad M, Doranehgard MH, et al. Optimal offering and bidding strategies of renewable energy based large consumer using a novel hybrid robust-stochastic approach. J Cleaner Prod 2019;215:878–89.
[6] Liu Yan, Liu Shu, Zhang Lihong, Cao Fuyi, Wang Liming. Optimization of the yaw control error of wind turbine. Front Energy Res 2021;9:P1–P10.
[7] Dazhong Wu, Xiaowei Wang. Research on a fuzzy control algorithm for photovoltaic MPPT. Acta Sol Energy Sin 2011;32(06):808–13.
[8] Pradhan R, Subudhi B. Double integral sliding mode MPPT control of a photovoltaic system. IEEE Trans Control Syst Technol 24(1):285–92.
[9] Xuanju Dang, Yang Yang, Hui Jiang, Jingjing Li. MPPT control with adaptive step size disturbance observation method based on incomplete differentiation. Acta Sol Energy Sin 2016;37(12):3022–9.
[10] Jize Tang, Congling Wang, Xuefa Fang. An implementation strategy of MPPT based on conductance increment method. Power Electron Technol 2011;45(04):73–5.
[11] Shaowu Li, Xianwen Gao. A VWP interval fuzzy MPPT control strategy for photovoltaic system. Acta Sol Energy Sin 2016;37(05):1167–73.
[12] Qing Zhu, Xing Zhang, Chun Liu. Research on particle swarm optimization MPPT algorithm based on voltage window restriction. Acta Sol Energy Sin 2016;37(06):1379–86.
[13] Yanwei Zhu, Xinchun Shi, Yangqing Dan, Peng Li, Wenying Liu, debing Wei, et al. Application of particle swarm optimization algorithm in multi peak maximum power point tracking of photovoltaic array. Chin J Electr. Eng. 2012;32(04). 42-48 + 20.
[14] Fang Xu, Ren Zhang, Lebin Wu, Hongwei Xu. Application of adaptive BP neural network in photovoltaic MPPT. Acta Sol Energy Sin 2012;33(03):468–72.
[15] Biwu Fang, Dichen Liu, Bo Wang, Bingke Yan, xunting Wang. Short term wind speed prediction based on LSSVM optimized by wavelet transform and improved firefly algorithm. Power Syst Prot Control 2016;44(08):37–43.
[16] Siqing Sheng, Yuliang Chen. Novel variable step incremental conductance MPPT strategy based on power prediction. Power Syst Prot Control 2017;45(23):42–8.
[17] Xu F. A MPPT control for photovoltaic power system based on the fuzzy control and variable step length disturbance observation method of power prediction. Comput Meas Control 2014;22. 414-416+430.
[18] Hongwei Xu, Libin Zhang, Fang Xu, Ren Zhang, Keyong Hu. Research on MPPT method of photovoltaic cells based on power prediction and voltage compensation. Acta Sol Energy Sin 2013;34(09):1599–605.